Topics in Catalysis
https://doi.org/10.1007/s11244-021-01530-0

ORIGINAL PAPER

Promotion of Oxygen Evolution Activity of Co-Based Nanocomposites by Introducing Fe^{3+} Ions

Xue Bai[1] · **Jingqi Guan**[1]

Accepted: 2 November 2021

Abstract
Improvement of the catalytic performance of oxygen evolution reaction (OER) is the key to the large-scale implementation of water electrolysis. Here, we report an efficient strategy to improve the OER activity of Co-based nanocomposite catalysts by adding Fe^{3+} ions into the electrolyte. The overpotential of cobalt tartrate annealed at 700 °C can be decreased from 360 to 329 mV by introducing 20 ppm Fe^{3+} into the alkaline electrolyte. Electrochemical measurements indicate that the introduction of Fe^{3+} can generate more efficient active sites by cooperation with Co species and promote OER kinetics, thus improving electrocatalytic performance.

Keywords Carbonous material · Cobalt · Fe-doping · Oxygen evolution reaction · Tartaric acid

1 Introduction

Accelerated consumption of fossil fuels accompanied by releasing vast quantities of carbon dioxide into the atmosphere, resulting in serious environmental degradation, which forces us to seek renewable and eco-friendly energy resources to replace the fossil fuels [1]. Hydrogen is one of the eco-friendly renewable energy carriers, which was mainly produced by oil cracking, natural gas reformation, and water electrolysis [2, 3]. Water splitting powered by renewable electricity resources provides one of the best methods for generating renewable and eco-friendly high-purity hydrogen [4]. However, high overpotentials required to initiate water electrolysis at appropriate rates with low power efficiency are the main issues for industrial brine electrolysis [5]. Therefore, it is urgently needed to develop high-efficiency catalysts to facilitate the sluggish oxygen evolution reaction (OER) and to improve energy efficiency [6].

Transition metal cobalt-based oxides and (oxy)hydroxides provide many interesting properties such as good electrical conductivity, excellent stability, and inexpensive availability for their facile synthesis [7]. Owing to their novel structural and physicochemical characteristics, cobalt oxide-based catalysts have been widely used for the OER [8, 9]. For instance, Markovic et al. [10] found that the trend in OER reactivity on 3*d*-M hydr(oxy)oxides was followed: Ni > Co > Fe > Mn. Wang et al. [11] created oxygen vacancies on Co_3O_4 surface by a plasma engraving strategy, which exhibited an overpotential (η_{10}) of 300 mV at 10 mA cm^{-2}, smaller than that on commercial Co_3O_4. Cao et al. [12] created in situ CoO_x species on the surface of Co metal, which showed an η_{10} of 289 mV. For cobalt oxide-based catalysts, the η_{10} can be reduced by 50 mV with increasing in surface area by one order of magnitude [13].

Although cobalt oxide-based catalysts show good OER activity in alkaline media, they still exhibit inferior activity than iridium oxide-based catalysts [14]. Fe-doping is a very efficient strategy to enhance the electrocatalytic OER performance. For example, Wang et al. [15] found that α-$Co_4Fe(OH)_x$ nanosheets needed an η_{10} of 295 mV. Zhu et al. [16] synthesized ultrathin $FeCoO_x$ nanosheets, showing an η_{10} of 350 mV. Yeo et al. [17] found that the η_{10} of CoO_x decrease from 378 to 309 mV with the addition of Fe^{3+} into the alkaline electrolyte. By in situ X-ray absorption fine structure spectra, they proposed that Fe and Co sites might not be the active sites since their valence states did not change during OER, but the adsorbed Fe with O-vacancies should be the actual active centers since the coordination number of Fe–O decreased after Fe^{3+} ions were adsorbed onto the surface of CoO_x. Theoretical studies revealed that

✉ Jingqi Guan
guanjq@jlu.edu.cn

[1] Institute of Physical Chemistry, College of Chemistry, Jilin University, 2519 Jiefang Road, Changchun 130021, People's Republic of China

Published online: 09 November 2021

the theoretical overpotential of Fe-doped α-$Co(OH)_2$ was smaller than pristine α-$Co(OH)_2$ [15].

Although there are many reports about metal–organic framework-derived catalysts for OER, there are seldom studies about tartrate-derived carbon-based nanomaterials for OER and it is still not very clear how the OER activity of CoO_x was improved by introducing Fe^{3+} ions. Herein, we report superior OER electrocatalysts based on pyrolysis of cobalt tartrate. Inspired by the adsorption of Fe^{3+} ions onto the surface of CoO_x and a cooperation mechanism between Fe and Co during OER, we introduced a small quantity of Fe^{3+} into the electrolyte, and found that the OER activity can be significantly improved due to enhanced active sites and improved OER kinetics.

2 Experimental

2.1 Materials

Cobaltous chloride, ferric nitrate, tartaric acid, KOH, and *N*,*N*-dimethylformamide were s purchased from Sinopharm Chemical Reagent Co. Ltd. (Shanghai, China). N_2 (99.99 %) was purchased from Juyang Gas (Changchun, China).

2.2 Catalyst Preparation

We developed a solvothermal method to prepare cobalt tartrate (Co-TA). Typically, 0.75 mmol cobaltous chloride and 2.0 mmol tartaric acid were dissolved in 40 mL *N*,*N*-dimethylformamide, which was transferred into 50 mL Teflon autoclave and heated at 110 °C for 24 h. The obtained solid was annealed in N_2 at different temperatures for 2 h, which was named as CoO_x@C-T (T = 600, 700, 800, and 900 °C).

2.3 Physicochemical Characterization

The phase of the catalysts was identified by XRD with Cu Kα radiation (λ = 1.5418 Å). Scanning electron microscope (SEM) images were taken on a HITACHI SU8020 operated at 30 kV. The XPS analysis was carried out on a Thermo ESCALAB 250Xi. The C 1*s* peak position was selected at 284.6 eV.

2.4 Electrochemical Characterization

Electrochemical measurements were performed a three-electrode system (CHI. 760E). The as-obtained samples, saturated calomel electrode (SCE), and Pt sheet were used as the working electrode, reference electrode, and counter electrode, respectively. For OER measurement, the electrolytes included Fe-free 1.0 M KOH and 20 ppm Fe^{3+}-containing 1.0 M KOH (Fe source: ferric nitrate). In all measurements, the SCE was calibrated with respect to RHE according to the formula: E (RHE) = E (SCE) + 0.241 + 0.0591 pH. LSV curves were conducted with 90 % *i*R-compensation. The EIS measurements were investigated in the frequency from 100 kHz to 0.1 Hz.

3 Results and Discussion

3.1 Structural and Morphology Characterization

The structure of CoO_x@C-T was analyzed by XRD. As exhibited in Fig. 1a, carbon (2θ = 44.3 and 51.6°; PDF#80-0017), cobalt (2θ = 41.7, 44.8, 47.6, and 62.7°; PDF#05-0727), and Co_3O_4 (2θ = 38.5, 44.8, and 65.2°; PDF#42-1467) are the main species. According to Debye–Sherrer equation, the average particle size of CoO_x@C-600, CoO_x@C-700, CoO_x@C-800, and CoO_x@C-900 is 32.5, 34.2, 37.6, and 42.1 nm, respectively. SEM image of CoO_x@C-700 shows that irregular globular nanoparticles are formed (Fig. 1b). Element distribution in the CoO_x@C-700 is confirmed by STEM coupled energy-dispersive X-ray spectroscopy (EDS) element mapping (Fig. 2c and f), showing that C, O, and Co atoms are uniformly dispersed. The average elemental content of C, O, and Co is 75.4 mol%, 12.9 mol%, and 11.7 mol%, respectively. Combined with XRD analysis, the metal cobalt should be coated by carbon and Co_3O_4 shells.

The surface compositions and chemical state of Co in the CoO_x@C-700 are characterized by XPS. Figure 2a exhibits that the CoO_x@C-700 mainly contains C, O, and Co elements. The C 1*s* spectrum shows two characteristic peaks located at 284.6 eV and 285.6 eV, which can be assigned as C–C and C–O bonding, respectively (Fig. 2b). The Co $2p_{3/2}$ peak can be deconvoluted into three peaks at 778.6, 779.8, and 781.4 eV, attributed to Co^0, Co^{3+} and Co^{2+}, respectively (Fig. 2c) [18, 19]. The fitted XPS spectrum of C 1*s* shows three characteristic peaks centered at 529.9, 531.5, and 532.9 eV, assigned to Co–O, defective O sites, and –OH, respectively (Fig. 2d) [20–23].

3.2 OER Performance

The OER activity of CoO_x@C-T was first assessed in 1.0 M KOH. As revealed in Fig. 3a, CoO_x@C-700 exhibits an overpotential (η_{10}) of 360 mV at 10 mA cm^{-2}, smaller than CoO_x@C-600 (395 mV), CoO_x@C-800 (374 mV), and CoO_x@C-900 (422 mV). The CoO_x@C samples annealed at 600-900 °C show a similar Tafel slope (Fig. 3b), indicating that they have the same reaction path for OER. Compared with CoO_x@C-600, CoO_x@C-800, and CoO_x@C-900, the enhanced OER activity of CoO_x@C-700 is due to more electrochemical active sites since the linear slope

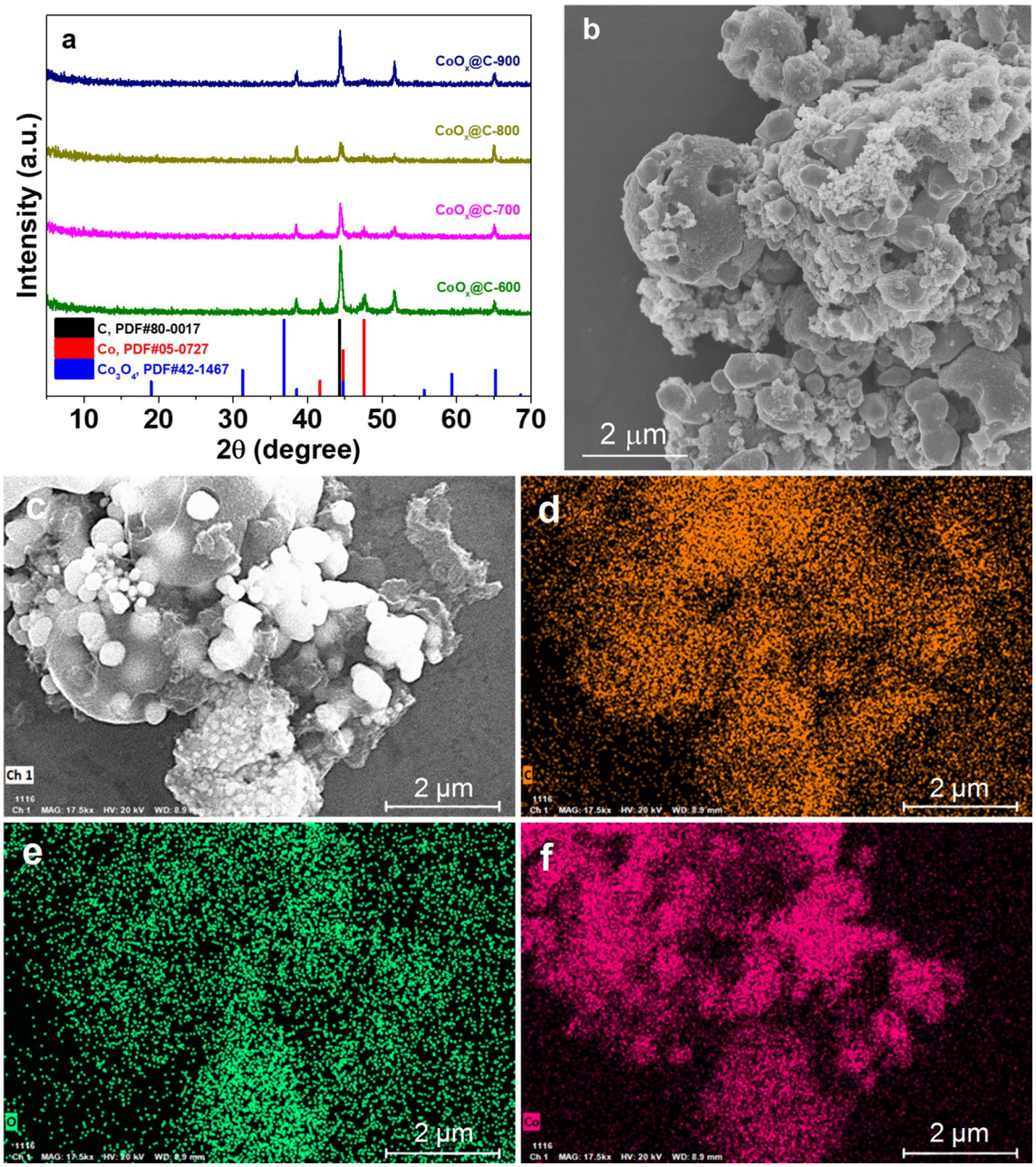

Fig. 1 **a** XRD patterns of CoO_x@C-T and reference samples. **b** SEM image of CoO_x@C-700. **c** SEM image of CoO_x@C-700 used in the EDS mapping test, and **d–f** the corresponding EDS mapping of C, O, and Co, respectively

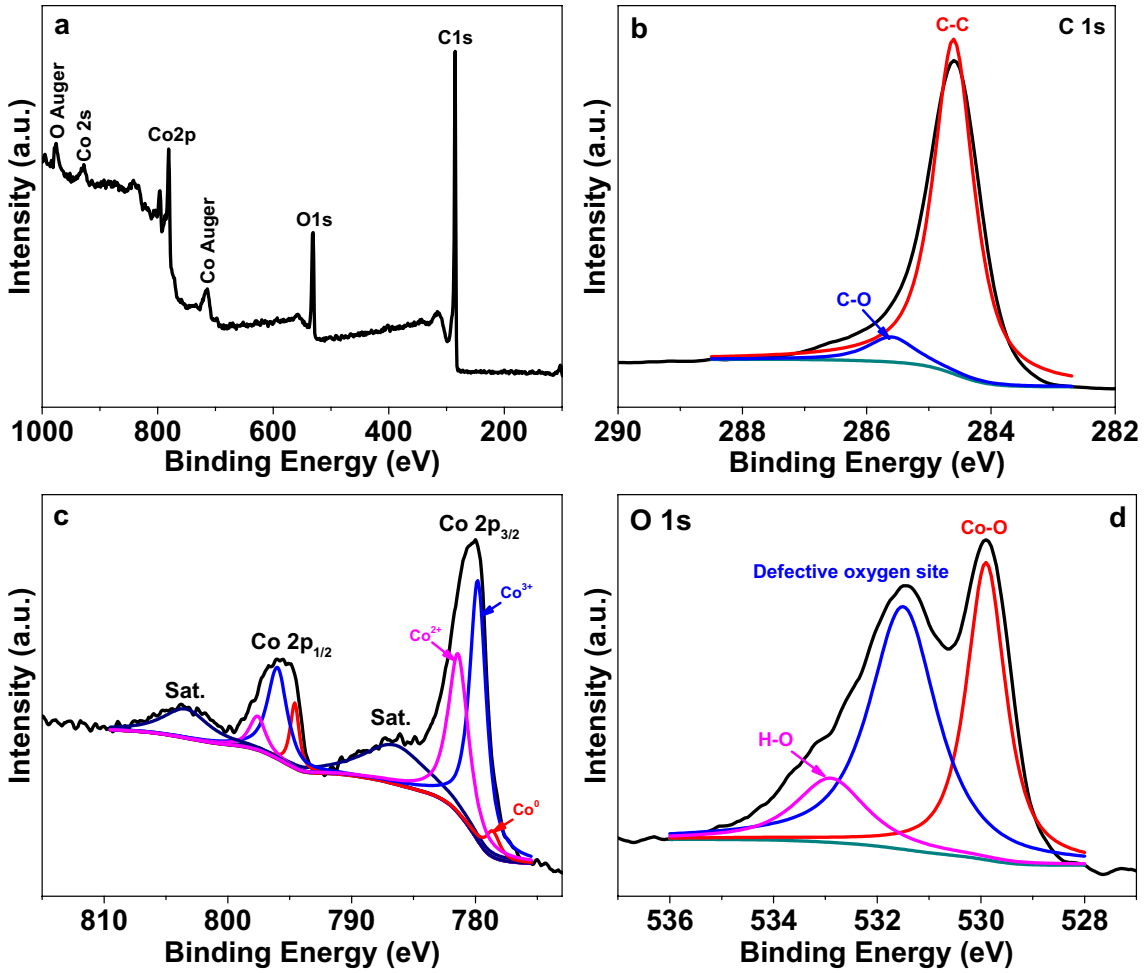

Fig. 2 **a** XPS survey spectrum of CoO_x@C-700 and XPS spectrum of **b** C 1*s*, (c) Co 2*p*, and (d) O 1*s*

of $\Delta j\left(\left|i_{charge} - j_{off\ charge}\right|\right)$ against the scan rates for CoO_x@C-700 is 16.3 mF cm^{-2} (Fig. 3c and d), larger than CoO_x@C-600 (1.3 mF cm^{-2}), CoO_x@C-800 (9.4 mF cm^{-2}), and CoO_x@C-900 (4.8 mF cm^{-2}).

The OER activity of CoO_x@C-T was further assessed in 1.0 M KOH with 20 ppm Fe^{3+}. To eliminate the error due to operation, the glassy carbon electrodes coated with CoO_x@C-T electrocatalysts after the OER measurement in 1.0 M KOH without Fe^{3+} were directly reused for the OER test in 1.0 M KOH with 20 ppm Fe^{3+}. By control experiment, we found that the concentration of Fe^{3+} (from 5 to 30 ppm) has no significant influence on the OER activity of CoO_x@C-700. As depicted in Fig. 4a, the η_{10} for CoO_x@C-600, CoO_x@C-700, CoO_x@C-800, and CoO_x@C-900 is 370, 329, 331, and 333 mV, respectively. Compared with that in 1.0 M KOH without Fe^{3+}, the OER activity of CoO_x@C-T in 1.0 M KOH with Fe^{3+} is significantly improved, which can be compared with those reported in previous studies (Table 1). In addition,

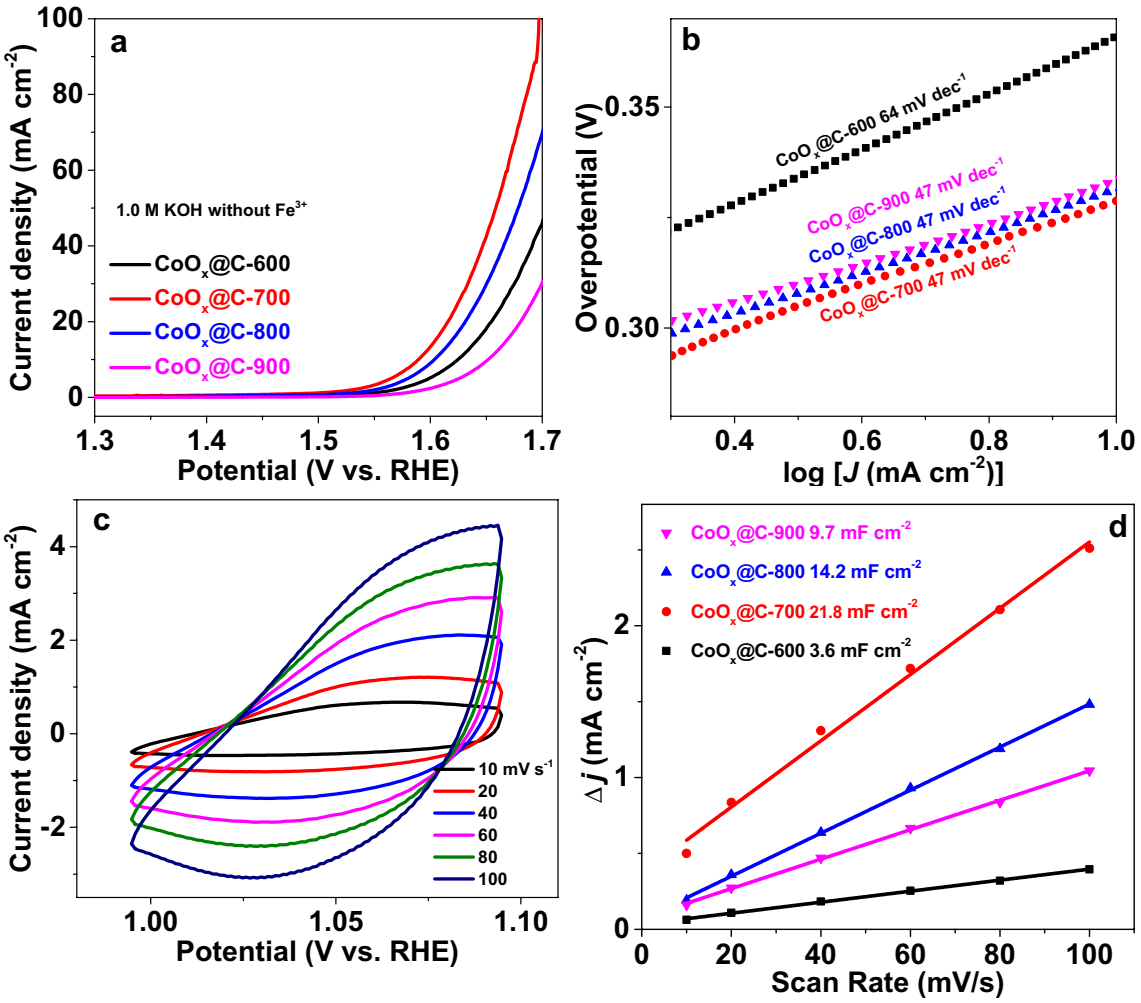

Fig. 3 **a** LSV curves. **b** Tafel slopes. **c** CV curves of CoO_x@C-700 and **d** capacitive j vs. scan rate

the Tafel slope of CoO_x@C-700 is only 47 mV dec^{-1} (Fig. 4b), like those of CoO_x@C-800 and CoO_x@C-900, indicating the same OER mechanism on these catalysts. Moreover, the CoO_x@C-T in 1.0 M KOH with Fe^{3+} show much smaller Tafel slopes than those in 1.0 M KOH without Fe^{3+}, suggesting that Fe and Co ions catalyze synergistically the OER. Furthermore, the linear slopes of Δj against the scan rates for the CoO_x@C-T in 1.0 M KOH with Fe^{3+} is greatly larger than those 1.0 M KOH without Fe^{3+}, suggesting enhanced electrochemical surface area (Fig. 4c and d). Since the electrodes in 1.0 M KOH with and without Fe^{3+} are the same, the capacitance should be approximately the same. The enhanced electrochemical surface area should be attributed to the increased active sites, further testifying that both Fe and Co ions participate in the OER. Additionally, the introduction of Fe^{3+} not only increases the number of active sites, but also improves the charge transfer as illustrated in Fig. 5, which favors

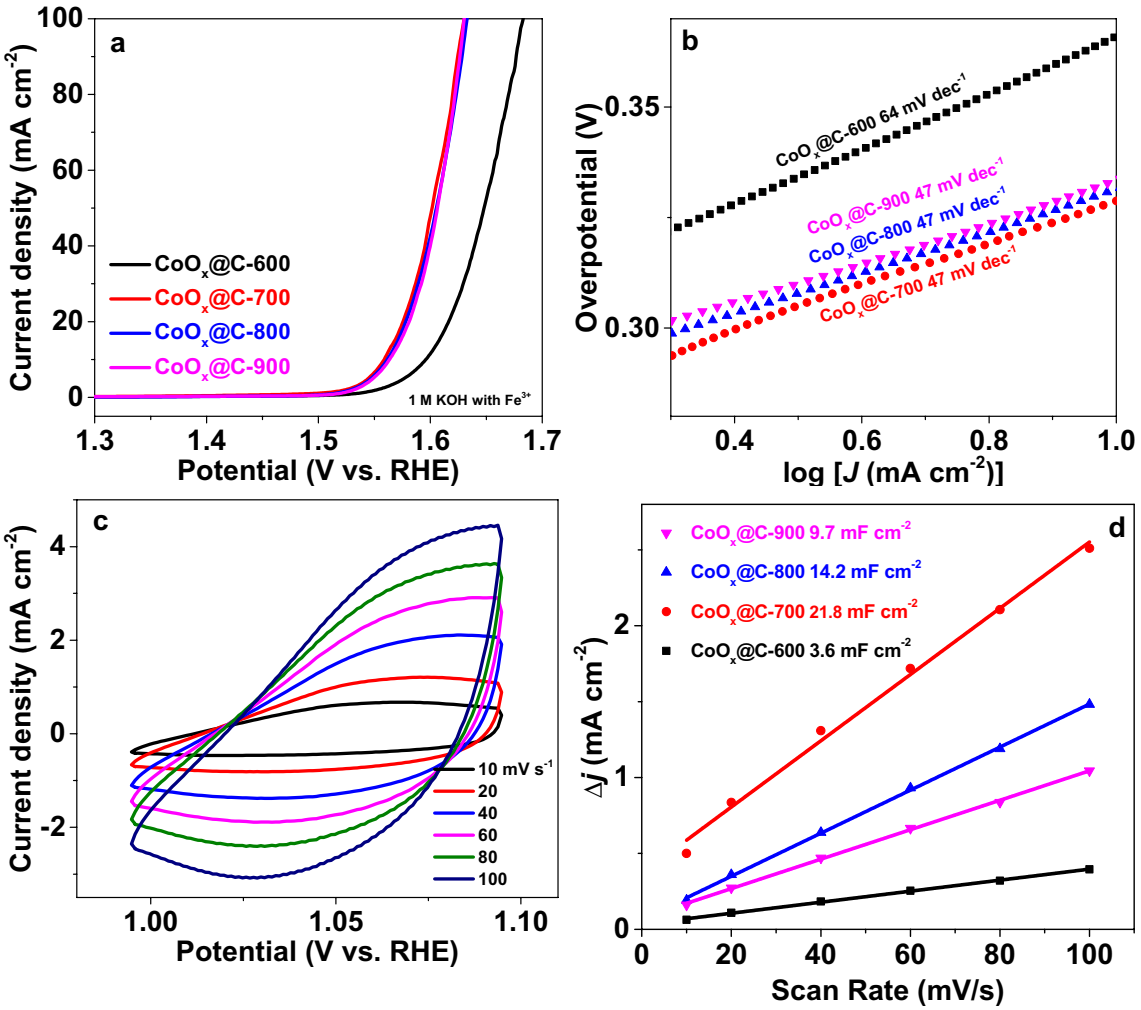

Fig. 4 **a** LSV curves in 1.0 M KOH with 20 ppm Fe^{3+}. **b** Tafel slopes. **c** CV curves of CoO_x@C-700 in 1.0 M KOH with 20 ppm Fe^{3+} and **d** capacitive j vs. scan rate

promotion of OER kinetics. Therefore, we propose that Fe and Co ions are the active sites for efficient OER.

The durability of CoO_x@C-700 was evaluated in 1.0 M KOH with Fe^{3+}. The multiple current steps of chronopotentiometry measurements show that the overpotential rapidly levels out and remains constant for the following 500 s when the current density is increased from 10 to 100 mA cm^{-2} (Fig. 6a). Moreover, there is no attenuation in the current density remained during 25 h at a constant potential of 1.56 V (Fig. 6b). The CoO_x@C-700 after stability test was analyzed by XRD, SEM, and XPS. From Fig. 7a, the structure of CoO_x@C-700 after OER test keeps unchanged. From Fig. 7b, the morphology of the CoO_x@C-700 after O_2 evolution was maintained constant. As demonstrated in Fig. 8a, besides C, O, and Co elements, K and Fe are also detected due to the absorption

Table 1 Comparison of OER performance of CoFe-based electrocatalysts

Catalyst	Electrolyte	η_{10} (mV)	Tafel slope (mV dec^{-1})	References
CoO_x@C-700 adsorbed with Fe^{3+}	1.0 M KOH	329	47	This work
α-$Co_4Fe(OH)_x$	1.0 M KOH	295	52	[15]
Fe-Co_3O_4	1.0 M KOH	280	55	[24]
CoFeS	1.0 M KOH	290	53	[25]
Fe–Co–P	1.0 M KOH	269	31	[26]
CFO1	1.0 M KOH	304	38	[27]
$CoFe_2O_4$	1.0 M KOH	378	55	[28]
$Co_{0.54}Fe_{0.46}OOH$	1.0 M KOH	390	47	[29]
FeCoS	1.0 M KOH	300	56	[30]
CoFe-CDs	1.0 M KOH	308	61	[31]
V_O-(Co, Fe)$_3O_4$/CC	1.0 M KOH	286	41	[32]
CoFe/NF	1.0 M KOH	220	40	[33]
Fe–Co_3O_4-0.6%	0.1 M KOH	410	78	[34]

on the surface. The Fe is mainly in the existence of Fe^{3+} (Fig. 8b). After OER electrocatalysis, the relative content of Co^{3+} is increased (Fig. 8c). Moreover, the relative content of defective oxygen sites is also enhanced due to the lattice oxygen involving in the reaction (Fig. 8d).

4 Conclusions

In summary, we have fabricated Co-based nanocomposite catalysts by a facile annealing method using a Co-based complex as the precursor. The obtained CoO_x@C-700 catalyst showed good OER activity with an η_{10} of 360 mV in Fe-free alkaline solution. The overpotential can be decreased to 329 mV in Fe^{3+}-containing KOH solution. The introduction of Fe^{3+} can cooperate with Co species to create more active sites and can accelerate the charge transfer ability to improve the OER performance. In addition, the CoO_x@C-700 exhibited excellent OER stability in the Fe^{3+}-containing KOH solution. The Fe^{3+}-doping approach described in this work may be applicable to actual water splitting system.

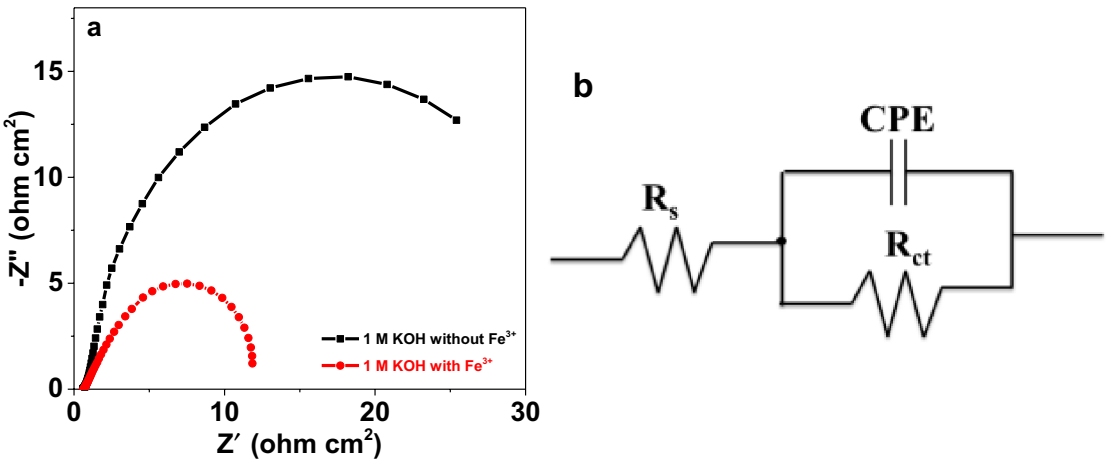

Fig. 5 **a** Nyquist plots of the EIS test for CoO_x@C-700 in 1.0 M KOH with and without Fe^{3+}. **b** The equivalent circuit used for fitting the Nyquist plots

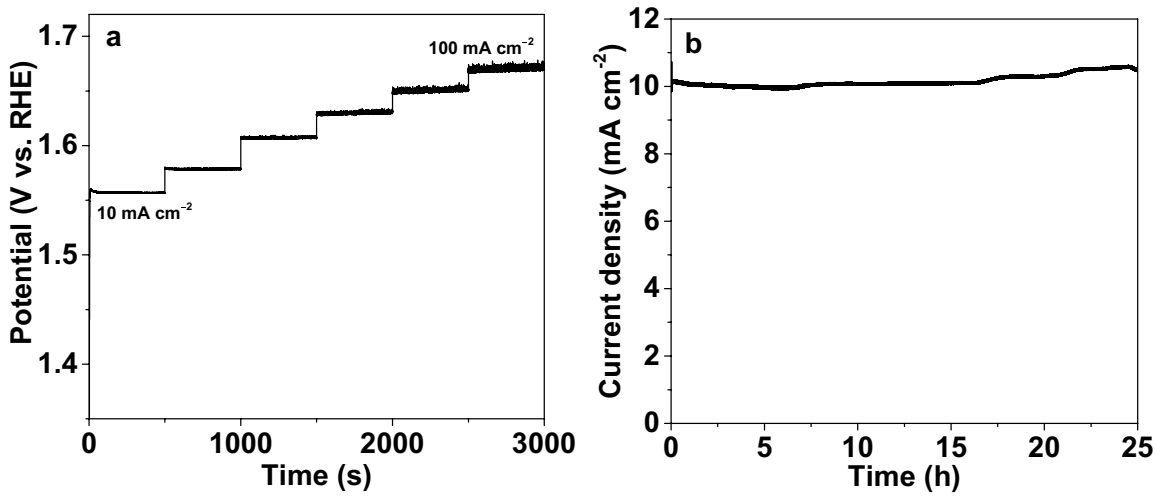

Fig. 6 **a** Multi-current electrochemical process of CoO_x@C-700. **b** Plot of current density versus time for CoO_x@C-700

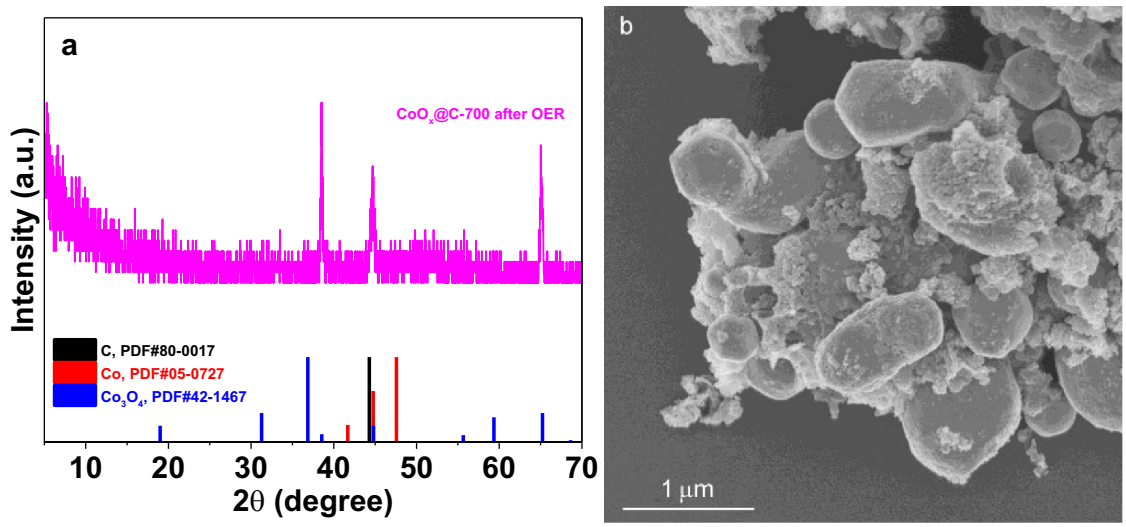

Fig. 7 **a** XRD pattern and **b** SEM image of CoO_x@C-700 after OER test

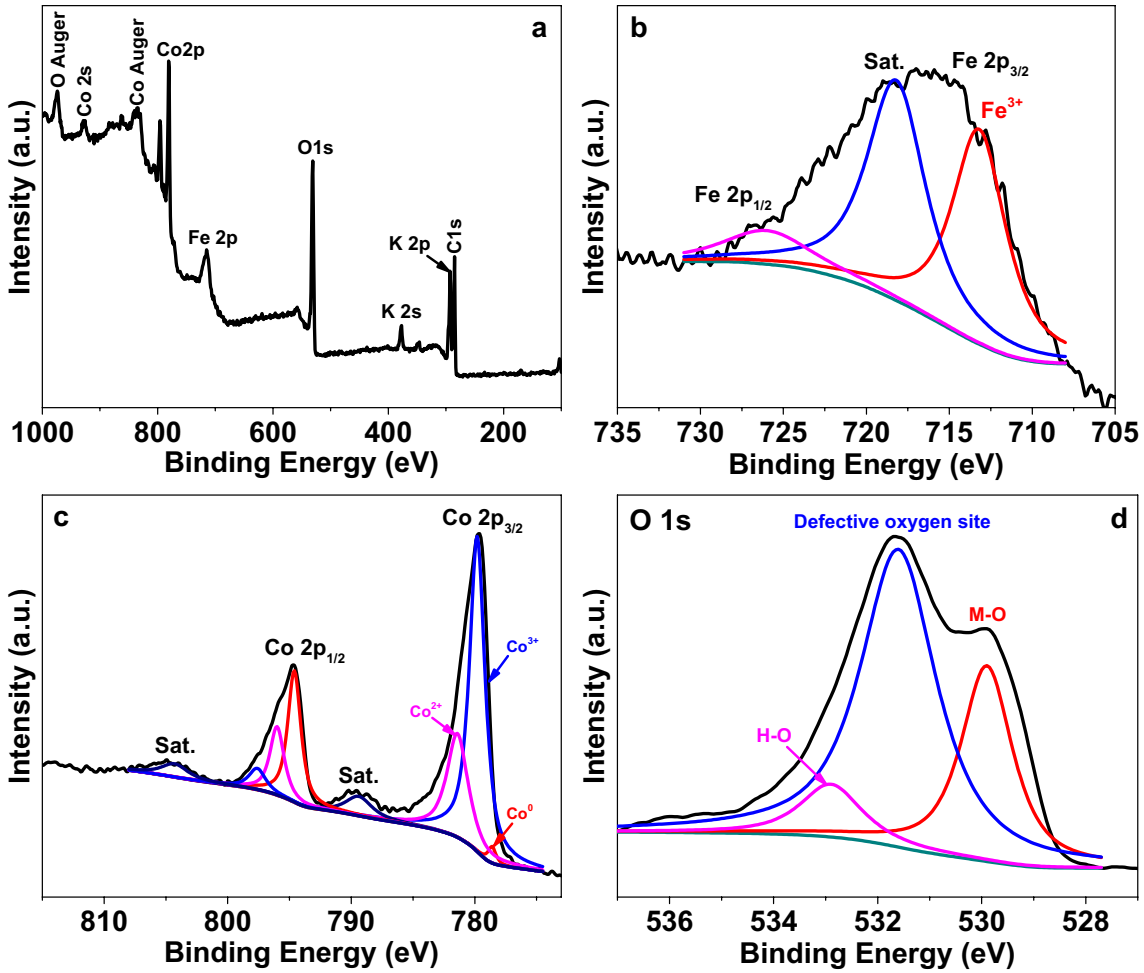

Fig. 8 **a** XPS survey spectrum of the used CoO_x@C-700 and XPS spectrum of **b** Fe 1*s*, (c) Co 2*p*, and (d) O 1*s*

Acknowledgements This work was supported by the National Natural Science Foundation of China (Grant No. 22075099).

References

1. Yu Z-Y, Duan Y, Feng X-Y, Yu X, Gao M-R, Yu S-H (2021) Clean and affordable hydrogen fuel from alkaline water splitting: past, recent progress, and future prospects. Adv Mater 33(31):2007100. https://doi.org/10.1002/adma.202007100
2. Yu M, Budiyanto E, Tuysuz H (2021) Principles of water electrolysis and recent progress in cobalt-, nickel-, and iron-based oxides for the oxygen evolution reaction. Angew Chem Int Ed 60:2–26. https://doi.org/10.1002/anie.202103824
3. Bakhtyari A, Makarem MA, Rahimpour MR (2019) Hydrogen production through pyrolysis. In: Lipman TE, Weber AZ (eds) Fuel cells and hydrogen production: a volume in the encyclopedia of sustainability science and technology, Second. Springer, New York, pp 947–973. https://doi.org/10.1007/978-1-4939-7789-5_956
4. Gao J, Tao H, Liu B (2021) Progress of nonprecious-metal-based electrocatalysts for oxygen evolution in acidic media. Adv Mater. https://doi.org/10.1002/adma.202003786
5. Zhang X-P, Wang H-Y, Zheng H, Zhang W, Cao R (2021) O–O bond formation mechanisms during the oxygen evolution reaction over synthetic molecular catalysts. Chin J Catal 42(8):1253–1268. https://doi.org/10.1016/s1872-2067(20)63681-6
6. Yao D, Gu L, Zuo B, Weng S, Deng S, Hao W (2021) A strategy for preparing high-efficiency and economical catalytic electrodes toward overall water splitting. Nanoscale 13(24):10624–10648. https://doi.org/10.1039/d1nr02307a
7. Badreldin A, Abusrafa AE, Abdel-Wahab A (2021) Oxygen-deficient cobalt-based oxides for electrocatalytic water splitting. ChemSusChem 14(1):10–32. https://doi.org/10.1002/cssc.202002002
8. Song Y, Xu B, Liao T, Guo J, Wu Y, Sun Z (2021) Electronic structure tuning of 2D metal (hydr)oxides nanosheets for electrocatalysis. Small 17(9):2002240. https://doi.org/10.1002/smll.202002240
9. Huang K, Sun Y, Zhang Y, Wang X, Zhang W, Feng S (2019) Hollow-structured metal oxides as oxygen-related catalysts. Adv Mater. https://doi.org/10.1002/adma.201801430
10. Subbaraman R, Tripkovic D, Chang K-C, Strmcnik D, Paulikas AP, Hirunsit P, Chan M, Greeley J, Stamenkovic V, Markovic NM (2012) Trends in activity for the water electrolyser reactions on 3d M(Ni,Co,Fe,Mn) hydr(oxy)oxide catalysts. Nat Mater 11(6):550–557. https://doi.org/10.1038/nmat3313

11. Xu L, Jiang Q, Xiao Z, Li X, Huo J, Wang S, Dai L (2016) Plasma-engraved Co_3O_4 nanosheets with oxygen vacancies and high surface area for the oxygen evolution reaction. Angew Chem Int Ed 55(17):5277–5281. https://doi.org/10.1002/anie.201600687
12. Qi J, Zhang W, Cao R (2017) Aligned cobalt-based Co@CoO_x nanostructures for efficient electrocatalytic water oxidation. Chem Commun 53(66):9277–9280. https://doi.org/10.1039/c7cc04609j
13. Deng X, Tueysuez H (2014) Cobalt-oxide-based materials as water oxidation catalyst: recent progress and challenges. ACS Catal 4(10):3701–3714. https://doi.org/10.1021/cs500713d
14. Li Y, Sun Y, Qin Y, Zhang W, Wang L, Luo M, Yang H, Guo S (2020) Recent advances on water-splitting electrocatalysis mediated by noble-metal-based nanostructured materials. Adv Energy Mater 10(11):1903120. https://doi.org/10.1002/aenm.201903120
15. Jin H, Mao S, Zhan G, Xu F, Bao X, Wang Y (2017) Fe incorporated alpha-Co(OH)(2) nanosheets with remarkably improved activity towards the oxygen evolution reaction. J Mater Chem A 5(3):1078–1084. https://doi.org/10.1039/c6ta09959a
16. Zhuang L, Ge L, Yang Y, Li M, Jia Y, Yao X, Zhu Z (2017) Ultrathin iron–cobalt oxide nanosheets with abundant oxygen vacancies for the oxygen evolution reaction. Adv Mater 29(17):1606793. https://doi.org/10.1002/adma.201606793
17. Gong L, Chng XYE, Du Y, Xi S, Yeo BS (2018) Enhanced catalysis of the electrochemical oxygen evolution reaction by iron(III) ions adsorbed on amorphous cobalt oxide. ACS Catal 8(2):807–814. https://doi.org/10.1021/acscatal.7b03509
18. Li M, Bai L, Wu S, Wen X, Guan J (2018) Co/CoO_x nanoparticles embedded on carbon for efficient catalysis of oxygen evolution and oxygen reduction reactions. Chemsuschem 11(10):1722–1727. https://doi.org/10.1002/cssc.201800489
19. Wan S, Qi J, Zhang W, Wang W, Zhang S, Liu K, Zheng H, Sun J, Wang S, Cao R (2017) Hierarchical Co(OH)F superstructure built by low-dimensional substructures for electrocatalytic water oxidation. Adv Mater 29(28):1700286. https://doi.org/10.1002/adma.201700286
20. Dong C, Yuan X, Wang X, Liu X, Dong W, Wang R, Duan Y, Huang F (2016) Rational design of cobalt–chromium layered double hydroxide as a highly efficient electrocatalyst for water oxidation. J Mater Chem A 4(29):11292–11298. https://doi.org/10.1039/c6ta04052g
21. Zhang Q, Liu N, Guan J (2019) Charge-transfer effects in Fe–Co and Fe–Co–Y oxides for electrocatalytic water oxidation reaction. ACS Appl Energy Mater 2(12):8903–8911. https://doi.org/10.1021/acsaem.9b01938
22. Liu N, Guan J (2021) Core–shell Co_3O_4@ FeO_x catalysts for efficient oxygen evolution reaction. Mater Today Energy 21:100715. https://doi.org/10.1016/j.mtener.2021.100715
23. Li Y, Lu M, Wu Y, Ji Q, Xu H, Gao J, Qian G, Zhang Q (2020) Morphology regulation of metal–organic framework-derived nanostructures for efficient oxygen evolution electrocatalysis. J Mater Chem A 8(35):18215–18219. https://doi.org/10.1039/d0ta05866a
24. Pan S, Mao X, Yu J, Hao L, Du A, Li B (2020) Remarkably improved oxygen evolution reaction activity of cobalt oxides by an Fe ion solution immersion process. Inorg Chem Front 7(18):3327–3339. https://doi.org/10.1039/d0qi00385a
25. Zhou Y, Luo M, Zhang Z, Li W, Shen X, Xia W, Zhou M, Zeng X (2018) Iron doped cobalt sulfide derived boosted electrocatalyst for water oxidation. Appl Surf Sci 448:9–15. https://doi.org/10.1016/j.apsusc.2018.04.080
26. Zhang H, Zhou W, Dong J, Lu XF, Lou XW (2019) Intramolecular electronic coupling in porous iron cobalt (oxy)phosphide nanoboxes enhances the electrocatalytic activity for oxygen evolution. Energy Environ Sci 12(11):3348–3355. https://doi.org/10.1039/c9ee02787d
27. Lyu F, Bai Y, Wang Q, Wang L, Zhang X, Yin Y (2019) Coordination-assisted synthesis of iron-incorporated cobalt oxide nanoplates for enhanced oxygen evolution. Mater Today Chem 11:112–118. https://doi.org/10.1016/j.mtchem.2018.10.010
28. Budiyanto E, Yu M, Chen M, DeBeer S, Rüdiger O, Tüysüz H (2020) Tailoring morphology and electronic structure of cobalt iron oxide nanowires for electrochemical oxygen evolution reaction. ACS Appl Energy Mater 3(9):8583–8594. https://doi.org/10.1021/acsaem.0c01201
29. Zhang X, An L, Yin J, Xi P, Zheng Z, Du Y (2017) Effective construction of high-quality iron oxy-hydroxides and Co-doped iron oxy-hydroxides nanostructures: towards the promising oxygen evolution reaction application. Sci Rep 7:43590. https://doi.org/10.1038/srep43590
30. Lalwani S, Joshi A, Singh G, Sharma RK (2019) Sulphur doped iron cobalt oxide nanocaterpillars: an electrode for supercapattery with ultrahigh energy density and oxygen evolution reaction. Electrochim Acta. https://doi.org/10.1016/j.electacta.2019.135076
31. Yang M, Feng T, Chen Y, Zhao X, Yang B (2019) Ionic-state cobalt and iron co-doped carbon dots with superior electrocatalytic activity for the oxygen evolution reaction. ChemElectroChem 6(7):2088–2094. https://doi.org/10.1002/celc.201900423
32. Liu F, Jin W, Li Y, Zheng L, Hu Y, Xu X, Xue Y, Tang C, Liu H, Zhang J (2020) Defect-rich (Co, Fe)$_3O_4$ hierarchical nanosheet arrays for efficient oxygen evolution reaction. Appl Surf Sci. https://doi.org/10.1016/j.apsusc.2020.147125
33. Babar P, Lokhande A, Shin HH, Pawar B, Gang MG, Pawar S, Kim JH (2018) Cobalt iron hydroxide as a precious metal-free bifunctional electrocatalyst for efficient overall water splitting. Small. https://doi.org/10.1002/smll.201702568
34. Swaminathan J, Puthirath AB, Sahoo MR, Nayak SK, Costin G, Vajtai R, Sharifi T, Ajayan PM (2019) Tuning the electrocatalytic activity of Co_3O_4 through discrete elemental doping. ACS Appl Mater Interfaces 11(43):39706–39714. https://doi.org/10.1021/acsami.9b06815